



# Integrated microfluidic device for single-cell trapping and spectroscopy

C. Liberale<sup>1</sup>, G. Cojoc<sup>2\*</sup>, F. Bragheri<sup>3‡</sup>, P. Minzioni<sup>3</sup>, G. Perozziello<sup>2</sup>, R. La Rocca<sup>1</sup>, L. Ferrara<sup>1,3</sup>, V. Rajamanickam<sup>1</sup>, E. Di Fabrizio<sup>1,2</sup> & I. Cristiani<sup>3</sup>

<sup>1</sup>KAUST (King Abdullah University of Science and Technology), PSE and BESE divisions, Jeddah, Saudi Arabia, <sup>2</sup>BioNEM Lab, Dipartimento di Medicina Sperimentale e Clinica, Università Magna Graecia di Catanzaro, 88100 Catanzaro, Italy, <sup>3</sup>Dipartimento di Ingegneria Industriale e dell'Informazione, Università di Pavia, Via Ferrata 1, 27100 Pavia, Italy.

**Optofluidic microsystems are key components towards lab-on-a-chip devices for manipulation and analysis of biological specimens. In particular, the integration of optical tweezers (OT) in these devices allows stable sample trapping, while making available mechanical, chemical and spectroscopic analyses.**

At the state-of-the-art, optical traps can be generated inside a microfluidic device either through “standard” OT obtained by tightly focused free-space laser beams or by OT based on counter-propagating beams.

Here we show a novel and fully-integrated system relying on miniaturized fibre-based OT that achieves stable 3D-trapping through micro-prisms beam deflectors fabricated by two-photon lithography. We then demonstrate its use for fluorescence and Raman measurements of single cells.

The proposed microsystem offers manipulation and analyses capabilities, while guaranteeing high flexibility and cell-safety, and allows to easily add multiple optical traps in Lab on chip miniaturized devices for analysis of biological and chemical samples.

With the advent of single-cell techniques and the ability to realize lab-on-chip devices based on a microfluidic network, the possibility of making real “cellular medicine” is becoming more than concrete<sup>1,2</sup>.

At the same time, the use of optical tweezers (OT) is increasingly applied in many laboratories around the world for contactless stable trapping and manipulation of live cells and has enabled obtaining fundamental results in several research fields, unveiling the molecular interactions in complex systems like proteins, DNA, cell membrane etc.<sup>3–5</sup>.

As a consequence, a growing interest is being attracted by the combination of OT in microfluidic systems, as it enables the realization of devices for biological analysis with enhanced sensitivity<sup>6,7</sup> and additionally paves the way to the conception of new measurement techniques for cell biology<sup>8</sup>. Moreover, this has the potential to have an important impact in biotechnological research, representing a key building block for realization of microfluidic flow cytometers<sup>9,10</sup> and cell sorters<sup>7,11</sup>. Indeed, by stabilizing the sample position, it will enhance the sensitivity of measurements requiring long integration times, as when collecting Raman scattering<sup>12</sup> or cell fluorescence with a very low expression of the stained molecules.

The interest in this approach is also motivated by the consideration that there is a full geometrical and hydrodynamic compatibility between optical tweezers and microfluidics. Furthermore, hydrodynamic forces in a laminar flow have the same order of magnitude of forces produced by optical tweezers (tens of picoNewton)<sup>13</sup>.

However, at the state of the art, the use of OT inside a lab-on-chip apparatus presents some criticalities, and it is mainly implemented with bulky microscopes<sup>6,7,10</sup> or by counter-propagating beams<sup>8,14–16</sup>.

In microscope-based OT, optical trapping is achieved by tightly focusing a laser through a high numerical aperture (NA) objective. These systems are very effective, but require critical alignment and large apparatus and, as a consequence, have not had a wide acceptance in biological laboratories. In addition, the use of tightly focused beams can induce thermal damage affecting the viability of specimen under test<sup>17</sup>. Finally, the limited field of view provided by high NA objectives can be a strong limitation, when analyzing a biological process within the size scale usually provided by a microfluidic circuit.

Instead, a combination of OT and microfluidic circuits with a fully-integrated approach will solve many of the previous issues, and it would open the use of these powerful devices also to non-OT-specialized personnel. Owing to the importance of this approach, several solutions have been proposed in the past and they are all based on the same principle, in which the traps were obtained by counterpropagating beams delivered by optical fibres or

SUBJECT AREAS:  
MATERIALS FOR OPTICS  
BIOTECHNOLOGY  
OPTICAL MANIPULATION AND  
TWEEZERS  
APPLIED PHYSICS

Received  
23 October 2012

Accepted  
28 January 2013

Published  
13 February 2013

Correspondence and  
requests for materials  
should be addressed to  
C.L. (carlo.liberale@iit.  
it)

\* Current address:  
Max Planck Institute of  
Molecular Cell Biology  
and Genetics MPI-  
CBG, Pfothenhauer str.  
108, Dresden 01307,  
Germany.

‡ Current address:  
Istituto di Fotonica e  
Nanotecnologie (IFN)  
– CNR, Dipartimento di  
Fisica, Politecnico di  
Milano, P.zza  
Leonardo da Vinci 32,  
20133 Milano, Italy.



waveguides, with working distances in the order of tens of microns, indeed at the same length scale of microfluidic channels.

Optical traps obtained through the insertion of dual counterpropagating fibre beams in a microfluidic circuit give rise to systems with a limited versatility: fibres need to be carefully mounted on planar substrates or grooves in order to guarantee a good alignment<sup>14</sup> and the set-up is often not reproducible with good accuracy. Alternative proposals involve integrated microfluidic systems containing vertical-cavity surface-emitting lasers (VCSEL) or GaAl/AlGaAs heterostructures that are able to trap and move microspheres and biological samples<sup>15</sup>, but they are quite complex to fabricate and offer a limited amount of available power. A different solution was recently reported in ref. 16 where counterpropagating beams are properly faced on microfluidic channels through integrated waveguides fabricated on a glass substrate, and in ref. 11, where a similar approach was used also to realize fluorescence-activated optical-sorting of cells. Anyway, the reported solutions based on counterpropagating beams, do not allow creation of two or more simultaneous trapping points close to each other, and the displacement of the trapping point, i.e. handling of the trapped specimen, is restricted to be along the direction of the laser-beam axis only. Moreover because of the hindrance caused by the two opposing optical waveguides, the exploitation of this geometry is very limited in circuits with complex branched microchannel network.

Nevertheless, there are no reasons to limit the future of optical manipulation to these approaches. In fact, by implementing OT on microprobes, new experimental possibilities open for the integration of optical traps with microfluidic systems, as well as for optical manipulation in different environments and, in a near future, for in-vivo single cell studies.

In this paper we demonstrate an alternative and powerful solution for the integration of OT inside a microfluidic system enabling also fluorescence and Raman microscopy and spectroscopy at the single-cell level.

The development of a highly efficient optical micro-tweezers ( $\mu$ OT) based on fibre bundles is the key step towards the achievement of such a goal. Beam shaping required to create the optical trap inside the microfluidic system is obtained by fabricating microprism reflectors by Two Photon Lithography (TPL) on the fibre facets<sup>18–20</sup>. This approach makes the device fabrication significantly easier compared to the focused-ion-beam technique employed in the earlier version of such  $\mu$ OT<sup>21</sup>, while improving the trapping performance.

In order to tailor  $\mu$ OT trapping capability with microfluidic system geometry we designed a device optimized to trap single cells (with a diameter up to 20  $\mu$ m) and with suitably long trapping distance (40–55  $\mu$ m, calculated as the distance from fibre-end to trapping point) still maintaining a good stiffness of the trap<sup>22</sup>.

The  $\mu$ OT was then integrated into a hybrid PMMA (Polymethyl methacrylate)-glass microfluidic circuit where the cells can flow with a controlled velocity and the  $\mu$ OT can trap a single cell and excite its Raman and fluorescence response. The chip is mounted on an inverted microscope that provides high resolution and high contrast imaging of the flowing cells. In principle, several  $\mu$ OT can be arbitrarily added to different sections or in correspondence of reservoirs present in the microfluidic chip, thus making possible monitoring the single cell response to different stimuli.

## Results

**Microtweezers fabrication.** Proper beam shaping enabling efficient trapping is achieved by combining the total-internal-reflection (TIR) at the interface between fibres and surrounding-medium with the utilization of a four-fibres bundle in which the cores are distributed according to an annular geometry (Fig. 1). The bundle was fabricated following the description reported in ref. 21. Specialty single-mode fibres (produced on request by J-Fiber, Jena.) with low index contrast (mode field diameter  $\approx$  9  $\mu$ m at  $\lambda = 1070$  nm, according to the results reported in ref. 22) and 80- $\mu$ m cladding-diameter were assembled, resulting in a miniaturized probe with an external diameter equal to 320  $\mu$ m.

As depicted in Fig. 1b the output beams are deflected by TIR occurring at the interface of four micro-prisms positioned on the fibre facets with the outer medium: the four deflected beams cross each other in the same spot, thus creating the optical trap.

The microprisms are fabricated by TPL: a femtosecond laser oscillator is directly focused inside a suitable resin deposited on the fibre-facets (Fig. 2a). The resin polymerizes through two-photon absorption only in the focal volume and the portion that is not polymerized can be easily removed through a solvent (Methods). TPL is reliable, fast and low cost and, owing to a computer-controlled piezoelectric positioning system, offers a great freedom in the fabrication of optical components with different shapes, which can also include curved surfaces on top of the fiber<sup>19,20</sup>. As a comparison to ref. 21, similar tweezers were obtained by the focused-ion-beam (FIB) milling technique that, although extremely effective, requires a complex and time-consuming procedure, does not allow the realization of structures with complex geometries and has high running costs. Furthermore, we note that the fabrication of reflectors, which protrude with respect to the fibre facet, allows obtaining devices with a longer trapping distance.

The prisms realized by TPL (see Fig. 2) were perfectly aligned on the fibre surface, so as to induce TIR at the first lateral surface of the prism (point K in the inset of Fig. 1b), yielding also normal incidence at the second lateral surface of the prism. Considering the polymerized resin refractive index (1.56) and water as outer medium, the minimum angle to have TIR is  $\alpha = 58.5^\circ$ , hence we chose to fabricate

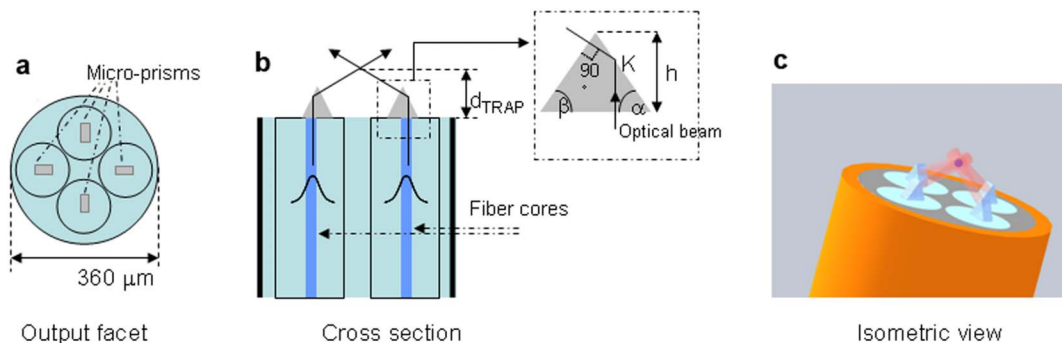


**Figure 1 | Schematics of the microtweezers structure.** (a) front-view of the output facet, showing the four fibres with microprisms. (b) cross-section of the fibre probe, the beams propagating in two symmetrically positioned fibres are reflected at the interface between microprisms and the outer medium; as reported in the inset, the prism angles are chosen so as to produce normal incidence on the second interface. (c) isometric representation of the optical tweezers trapping a particle.

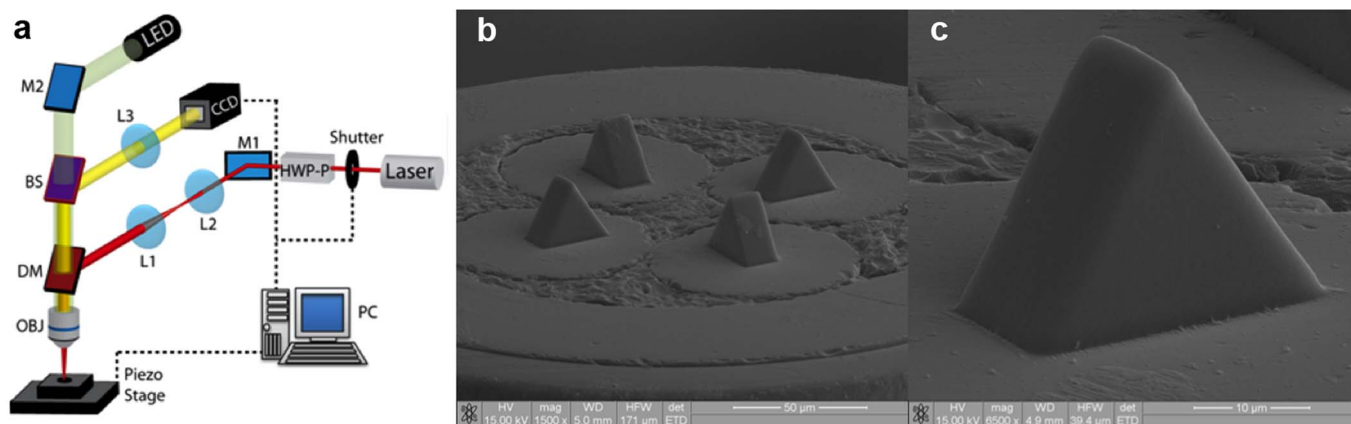


**Figure 2 | Two-photon lithography microprisms fabrication.** (a) Diagram of the experimental TPL setup: HWP-P – variable attenuator; L1 and L2 lenses for beam expander; L3 imaging tube lens; BS – beam splitter, DM – dichroic mirror and OBJ – microscope objective; M1 and M2 – mirrors. Details on the fabrication technique are reported in the methods section. (b) SEM image of the end-face of the fibre-tweezers. The prisms completely cover the fibres' core. (c) Detail of a single prism: the roughness of the surface is below 100 nm, thus not affecting the optical quality of the transmitted beam.

micro-prisms with  $\alpha = 60^\circ$  as a safety value to compensate for fabrication tolerances. With this design we calculated an effective NA = 1.15 and a trapping distance from the probe surface  $d_{\text{TRAP}} = 46 \mu\text{m}$ .

After fabrication, microprisms were inspected by using a scanning electron microscope (SEM). Figures 2b and 2c show the overall structure and the detail of a single prism, respectively. The surface exhibits a very good quality with a typical roughness below 100 nm. In the several runs of fabrication we found a spread in the actual values of the angles  $\alpha$  and  $\beta$  (see Fig. 1B) of  $\pm 1^\circ$ .

The optical properties of  $\mu\text{OT}$  were tested by an all fibre set-up (Fig. 3a and Methods). The radiation emitted by a Ytterbium doped fibre laser at  $\lambda = 1070 \text{ nm}$  was coupled to the four single-mode fibres composing the bundle with a  $1 \times 4$  fibre coupler, and the optical power distribution among the four fibres was finely tuned by means of variable optical attenuators.

After checking the convergence of the four beams, trapping capabilities of the  $\mu\text{OT}$  were verified by mounting the probe, held by a  $xyz$  micro-translator, parallel to the  $xy$  translation stage of an inverted microscope (Nikon TE2000). The fibre probe-end was placed on the object plane of a  $20\times$  objective while a CCD camera recorded the trapping action. As a first test, we deposited a drop of a water suspension of  $10 \mu\text{m}$  diameter polystyrene beads on a coverslip and we observed trapping and moving of single beads.

$\mu\text{OT}$  calibration was then carried out by video-tracking the Brownian motion of the trapped particle<sup>23</sup>. Performance of the  $\mu\text{OT}$  was evaluated by using polystyrene particles with a diameter of 7, 10 and  $15 \mu\text{m}$  (see Methods). Fig. 3b reports the values of stiffness per unit power in the direction perpendicular to the fibre probe axis, showing that the trap structure is ideally suited for particles in the size range from 10 to  $20 \mu\text{m}$  that matches the typical size of biological cells.

It is very important to notice that in this particle-size range  $\mu\text{OT}$  provides a trapping efficiency comparable to that of OT based on high-NA microscope objective<sup>24,25</sup>. In addition, in contrast to standard tweezers, the beams emitted by the fibres are not focused nor collimated, hence the intensity of the beams is very low ( $\approx 10^3 \text{ W/cm}^2$ ), thus minimizing any alteration of biological samples viability due to thermal effects induced by the trapping radiation.

We tested the trapping capabilities of  $\mu\text{OT}$  also with different biological samples, namely red blood cells (RBC) diluted in hypotonic or isotonic solution (see Fig. 4) and tumor cells (colon cancer cells) diluted in phosphate buffered saline solution. In both cases we were able to stably trap single cells by setting the power output at each prism at 5 mW.

The movie reported in Supplementary Video S1 shows a trapped RBC, moved inside the solution by translating the probe. It can be noticed that the trapping distance from the probe-end is quite large

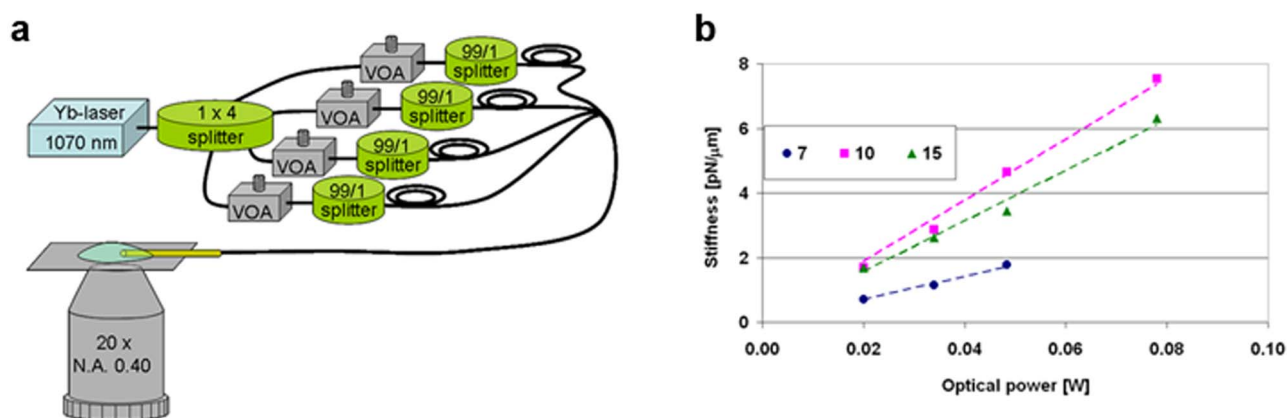


**Figure 3 | Characterization of the fibre tweezers trapping efficiency.** (a) all-fibre optical set-up exploited to test the trapping efficiency of the fibre tweezers. VOA: Variable optical attenuator, for sake of simplicity the 1% output of the 99/1 splitter is not shown in the scheme. (b) trapping stiffness, as a function of the optical power, considering polystyrene beads. The power-normalized stiffness is given by the slope of the linear fit, for each particle size. According to the collected data, the stiffness lower limit is about 94, 78 and  $35 \text{ pN } \mu\text{m}^{-1} \text{ W}^{-1}$  for beads with a diameter of 10, 15 and  $7 \mu\text{m}$ , respectively.

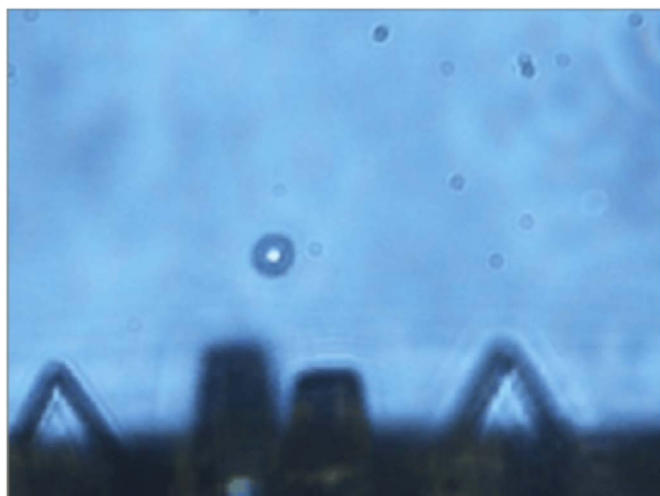


**Figure 4 | Red blood cell trapping and handling.** Frame taken from the video reported in Supplementary Video S1, showing the probe tip (with four protruding prisms) used to trap and move a red blood cell in hypotonic solution.

( $\approx 50 \mu\text{m}$ ), thus leaving a great degree of freedom in monitoring the cell and possibly illuminate it with additional optical beams for further analysis.

We also tested the trapping capabilities of  $\mu\text{OT}$  when using only two optical beams emitted by two opposite prisms. We alternatively switched off one couple of prisms and in both cases we could still observe stable trapping of RBC.

**On-chip trapping and spectroscopy.**  $\mu\text{OT}$  were then integrated in a microfluidic system in such a way as to enable trapping and analysis

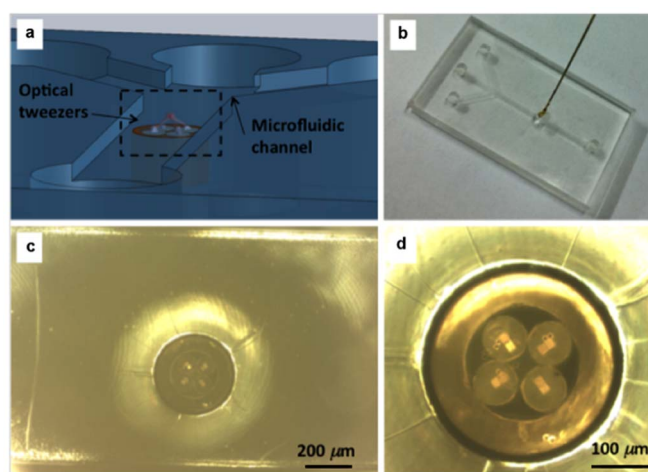


**Figure 5 |  $\mu\text{OT}$  integrated in a microfluidic chip.** (a) Isometric view of the optical tweezers integrated in the microfluidic system (the schematic diagram shows an overturned view of the top layer for in order to have a better visualization). (b) Top view picture of the device. (c) Zoomed picture of the optical tweezers inside the microfluidic channel (whose lateral walls are also visible at top and bottom of the picture). (d) Zoomed picture of the microprisms on the optical tweezers.

of biological specimen flowing inside the channel. The microfluidic device consists of one PMMA layer (2 cm wide, 3 cm long and 2 mm thick) bonded to a glass coverslip and includes a microfluidic channel (1 mm wide and  $60 \mu\text{m}$  deep), 3 inlets enabling hydrodynamic focusing of the flowing particle, 1 outlet and a calibrated hole for the integration of the  $\mu\text{OT}$  (Methods). The coverslip bottom layer offers full compatibility with standard microscope-based imaging

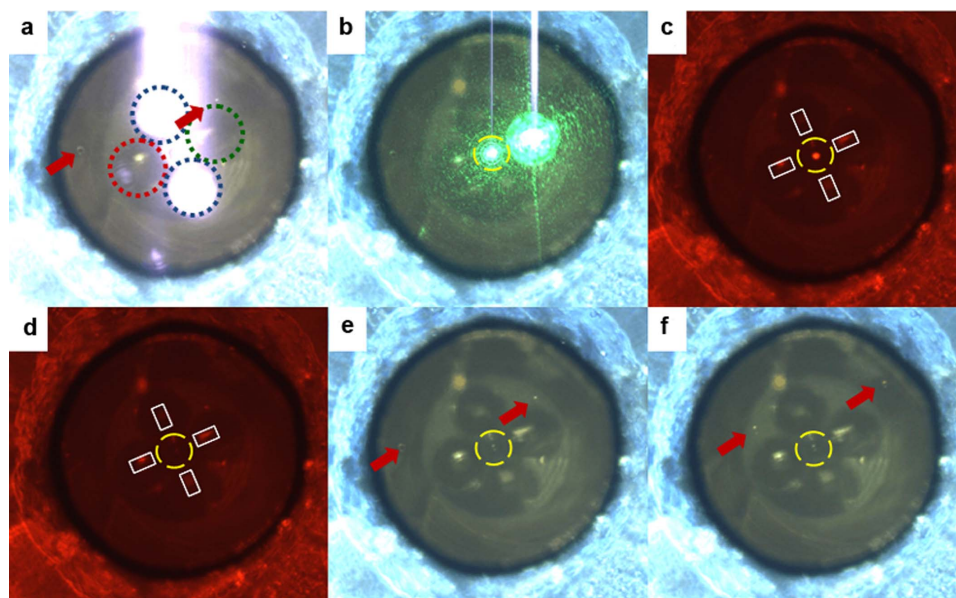


**Figure 6 | Fluorescence spectroscopy in the microfluidic integrated system.** Sequence of images obtained starting from the frames of Supplementary Video S2. (a) Front-view of the probe: the two fibres indicated by the blue dotted line emit the infrared radiation used to trap the particle. The fibre surrounded by the green circle is connected to the 532-nm laser source, while the one surrounded by the red circle is unused. Red arrows indicate the position of two non-trapped beads. (b) After inserting an IR-filter and switching on the 532-nm laser the green light scattered by the trapped particle (inside the yellow, dashed circle) is evident. (c) A long-pass filter is introduced in the light path to remove the 532-nm radiation from the image and the trapped bead ( $7.5 \mu\text{m}$  in diameter) shows an evident red fluorescence. (d) When the 532-nm laser is switched off the fluorescence disappear: the red light visible in the picture is given by coaxial white-light illumination used to illuminate the scene. (e) When the long-pass filter is removed, and the IR-filter is used, it is possible to observe the trapped bead in the centre of the yellow circle, as well as two additional beads indicated by the red arrows. (f) When the flow is restored the trapped bead remains stably trapped, while the other beads flow towards the upper right corner.

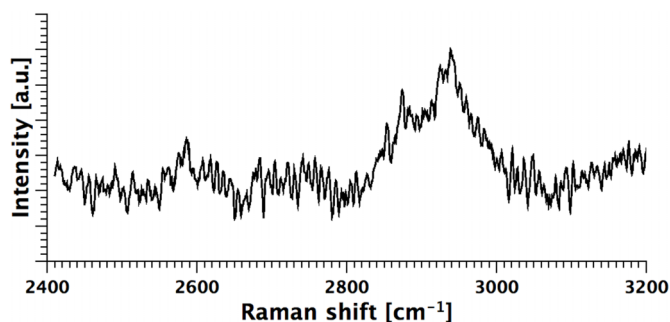


**Figure 7 | Raman signature of a cell optically trapped into the microfluidic channel.** Raman signature of a colon cancer cell in the C-H stretch Raman band, which is typically dominated by the lipidic and protein content. The Raman scattering has been collected through a microscope objective and measured by a commercial spectrometer.

techniques even with short working distance high-NA microscope objectives (see Fig. 5).

$\mu$ OT were mounted so that the optical trap was positioned about 10  $\mu$ m above the bottom surface of the channel, corresponding to the typical height at which most of the cells flow in stable regime conditions. We note that, from the detection viewpoint, our system is in fact identical to a fluorescence inverted microscope configuration, where the observed sample is within few microns from a coverglass and the microscope objective can be freely chosen by the operator.

First, we verified that the samples flowing in the micro-channel were easily and stably trapped by the  $\mu$ OT.

Additionally, to test the device capability to perform fluorescence spectroscopy analysis, we modified the optical set-up feeding the  $\mu$ OT as described in Methods. Fluorescent micro-beads (Bangs-Lab, FS06F/10007 532 nm/640 nm) diluted in water were flown inside the micro-chip. The radiation at 1070 nm emitted by two prisms was exploited to stably trap the selected beads, whereas green radiation at 532 nm was coupled in a third fibre of the bundle and then redirected by the prism towards the trapped particle. As shown in Fig. 6 (and Supplementary Video S2) once the bead is trapped, green light was switched on. After filtering out the green radiation by a notch filter, the red fluorescence of the beads can be easily recorded through the CCD camera. We note that the device operation is independent of the radiation wavelength and the prisms output is always aligned in such a way as to impinge on the trapped sample.

As a final test, we recorded the Raman signature of live cells trapped in the microfluidic channel. The samples were excited by a 633 nm laser, coupled into one of the four fibres, while the Raman scattering was collected by a microscope objective (Nikon 60x, 0.95 NA) and sent for spectral analysis to the spectrometer of a commercial Raman microscope (InVia Renishaw). As an example, the Raman signature of a colon cancer cell in the C-H stretch Raman band, which is typically dominated by the lipidic and protein content<sup>26</sup>, is shown in Fig. 7.

Regarding the potential downscaling of the proposed device, we point out that the microchannel lateral size can be, in principle, reduced to be equal to the size of the fiber optical tweezers probe. In turn, our fiber optical tweezers probe could be reduced in size by reducing the diameter of the fibers' claddings and the size of the external capillary, being the distance among the cores (around 100  $\mu$ m) the important parameter to be maintained.

We note that the proposed device paves the way to development of further on-chip analysis techniques: the capability to obtain a stable trap with just two prisms offers the chance to design two separate traps in different positions at the  $\mu$ OT output, thus making possible to simultaneously trap multiple cells at a close and controlled distance. Moreover, compared to the dual beam counterpropagating configuration, our microsystem allows the insertion, as a part of

the fibre bundle, of specialized optical fibres (e.g. for specific wavelengths, or having large cores for efficient scattered light collection) or even microcapillaries (e.g. to introduce a proper stimulus on a trapped cell).

The here reported device can be a key building block for the realization of microfluidic flow cytometers and cell sorters, when long integration times for the analysis require a stable position for the sample. At the same time, the device can be used as a tool for clinical assays. In fact, the sorted and trapped cells can be manipulated, subjected to stimuli of various nature or to drugs and can be monitored and analyzed by the same OT<sup>27,28</sup>.

## Discussion

We have presented a new approach to the development of microfluidic devices for lab-on-chip applications integrating optical trapping and manipulation capabilities. This achievement is made possible by the design and development of miniaturized optical tweezers enabling on-chip manipulation, Raman and fluorescence spectroscopy of single cells. The  $\mu$ OT fabrication technique, based on TPL, is simple, versatile, and allows the integration of additional mechanical and optical functions (like multiple traps and controlled microtranslations or microsurgery) leading to a powerful and multi-purpose probe. The presented device offers manipulation and analyses capabilities offered by high-NA microscope-objective OT, while preserving the full integration, flexibility and cell-safety of the OT based on counter-propagating beams. The efficient integration of microtweezers in a microfluidic circuit allows creating of a laboratory under the microscope allowing manipulation, treatment and analysis of single living cells. The versatility, low cost, ease of fabrication and assembly give to this system great potential as a general approach for isolating rare cells or observing the effects of local environmental changes for diagnosis or screening purposes.

## Methods

**Microprisms fabrication by two photon lithography.** The micro-prism fabrication is carried out by using the set-up shown in Fig. 2. A 100-fs pulsewidth, 80-MHz (pulse energy < 1 nJ) Ti:sapphire laser oscillator (Tsunami, Spectra Physics) is focused through a dry semi-apochromatic microscope objective (NA = 0.70). A proper fibre holder is mounted on a xyz piezo-stage with a 80  $\mu$ m travel range on all axes, for 3D position control.

The fibre holder is designed in such a way as to let the laser beam from the microscope objective to pass through a glass coverslip and then be focused on a droplet of photo-curable material in which the fibre bundle is immersed<sup>29</sup>. A precision linear translator controls the distance between the fibre and the coverslip. A commercial UV curing adhesive (NOA 63, Norland) was chosen as a photopolymer for fabrication due to its good adhesion to glass, easy processing, refractive index comparable to that of optical fibres, and very low cost.

The laser wavelength is tuned at 720 nm and the laser power is set to about 4 mW at the sample plane. The beam is expanded by a telescope, to obtain overfilling of the focusing microscope objective, and it is then reflected by a 45° short-pass dichroic mirror, which is almost transparent in the visible part of the spectrum, for imaging purposes. The image of the sample is taken through a CCD camera thus allowing fibre alignment, focusing and real-time monitoring of the polymerization process. A computer-driven mechanical shutter is used to control the exposure time for each pixel. The exposure time needed to fabricate a single microprism is typically around 10 min; as a comparison about half an hour was generally required to drill each hole by FIB in ref. 21. After the completion of exposure for the four micro-prisms, the fibre bundle is retracted from the droplet and the unexposed photoresist is removed with acetone and methanol, leaving the fabricated 3D structure attached to the fibre top.

The final microprisms are 25  $\mu$ m high and with a base area guaranteeing the collection of more than 95% of the power emitted by the fibres.

**Experimental set-up for optical trapping.** The quality of the fabricated probes was assessed by means of the all-fibre setup shown in Figure 3. The 1070 nm radiation emitted by a Ytterbium-doped fibre laser (IPG Fibertech) is coupled to the four tweezers input fibres by means of a 1 x 4 fibre-optic coupler; the optical power at each branch is finely tuned by means of variable optical attenuators and monitored through the 1% port of a 99%-1% coupler inserted in each branch. Trapping and manipulation capability are tested by matching the power output from each prism starting from a value of 3 mW, allowing an extremely compact and stable set-up to be obtained.

**Optical set-up for fluorescence and Raman spectroscopy.** For the spectroscopy measurements, the microfluidic system was mounted on the object plane of an



inverted microscope (TE2000, Nikon), and the experiments were carried out by slightly modifying the all-fibre optical setup. The 1070 nm trapping radiation was coupled to only two of the four fibres composing the tweezers, corresponding to two opposing micropipettes. For fluorescence spectroscopy measurements, a 532 nm radiation of 50 mW emitted by a frequency-doubled Nd: YAG laser source was coupled to one of the fibres composing the bundle. Experiment has been performed first by trapping a 7.5  $\mu\text{m}$  fluorescent polystyrene beads, hence by switching on the excitation radiation at 532 nm. Fluorescence emitted at 640 nm was collected through a CCD camera (Nikon) connected to the microscope. On the other hand, the Raman signatures of single trapped cells were measured by exciting the sample at 633 nm through one of the fibres of the bundle, as for fluorescence excitation. The incident power at the sample plane is 3 mW. The Raman scattering from sample was collected by a 60x, 0.95 NA microscope objective and directed to the spectrometer of a commercial (InVia, Renishaw) Raman microscope.

**Measurement of the trap stiffness.** The stiffness calibration is based on the study of the Brownian motion of a stably trapped particle. The bead was held in the trap for a couple of minutes and a video was recorded at a frame rate of 16 fps. The video was then analyzed and the coordinates of the bead's position in each frame were extracted.

The optical potential was then reconstructed using Boltzmann statistics, yielding a continuous profile of the trapping potential. Indicating with  $\rho(x)$  the probability density of the 1D particle position, which was derived by experimental acquisition, the shape of the trapping potential could be obtained as  $\ln[1/\rho(x)]$ .

By fitting the potential well with a parabola, the trap stiffness was then retrieved. This measurement provides lower bound to the restoring force applied by the optical trap to the trapped particle under the hypothesis of a parabolic potential well.

As the stiffness thus calculated is linearly dependent on the optical power  $P$  we define a power-normalized stiffness as  $k/P$ , which is thus expressed in  $\text{pN } \mu\text{m}^{-1} \text{W}^{-1}$  and is related only to the beam geometry and to the properties of the trapped particle. Comparing the obtained values with those reported in ref. 24,25 we find that the proposed tweezers have almost the same power-normalized stiffness of those based on highly-focused beams, if particles with a diameter of about 10 microns are considered.

**Integration of microtweezers with the microfluidic chip.** The microfluidic channels were fabricated by photolithography on top of a glass cover slip (0.16 mm tick, 24 mm wide and 40 mm long from Knittel Glaser) laminated with a 50  $\mu\text{m}$  thick dry photoresist (Ordyl SY300 from Elga Europe). The channels were sealed with a 2 mm thick PMMA lid by solvent assisted bonding<sup>30</sup>. The inlets and outlets and the optical fibre insert hole were fabricated by micromilling (Mini Mill GX from Minitech Machinery, Norcross, Georgia, United States) on the PMMA lid prior to bonding. The microfluidic channel was 60  $\mu\text{m}$  deep, 1 mm wide and 2 cm long. The 3 inlets and one outlet, having a diameter of 2 mm, were machined in correspondence of the end of the fluidic channel. The calibrated hole of 360  $\mu\text{m}$  in diameter for fibre insertion was fabricated in the middle of the microfluidic channel.

Before bonding, the PMMA and the glass layers were cleaned by ultrasound bath in deionized water for 5 minutes. The bonding was a solvent assisted process consisting in: 1) placing the PMMA layers in Ethanol for 15 minutes; 2) Aligning and pressing the PMMA layer and the glass slide together at a pressure of 0.5 bar; 3) placing the pressed layers in the oven at 90°C for 30 minutes.

Before placing the PMMA layer in Ethanol, the optical fibre bundle was inserted in the calibrated hole of the top PMMA layer.  $\mu\text{OT}$  were optically aligned in order to level its end to the top surface of the microfluidic channel. Once aligned, epoxy glue was used to fix the fibre bundle, seal the channel, and give structural rigidity.

The inlets of the microfluidic channel were connected through silicone tubes to reservoirs containing the samples under test, whereas the outlet was connected to a waste reservoir. The tubes and the system were filled with PBS by means of a syringe. The flow was controlled by exploiting the communicating vessel principle: the pressure in the microchannel was tuned by changing the relative position in height between the input and output reservoirs, thus carefully driving the samples towards the trapping position.

1. El-Ali, J., Sorger, P. K. & Jensen, K. F. Cells on chips. *Nature* **442**, 403–411 (2006).
2. Psaltis, D., Quake, S. R. & Yang, C. Developing optofluidic technology through the fusion of microfluidics and optics. *Nature* **442**, 381–6 (2006).
3. Chiou, A. *et al.* Optical Trapping and Manipulation for Biomedical Applications. In L. Pavesi & P. M. Fauchet (Eds.) *Biophotonics*, 249–273 (Springer Berlin Heidelberg, 2008).
4. Neuman, K. C. & Block, S. M. Optical trapping. *Rev. Sci. Instrum.* **75**, 2787–809 (2004).
5. Cojoc, D. *et al.* Properties of the Force Exerted by Filopodia and Lamellipodia and the Involvement of Cytoskeletal Components. *PLoS ONE*, doi:10.1371/journal.pone.0001072 (2007).
6. Eriksson, E. *et al.* A microfluidic system in combination with optical tweezers for analyzing rapid and reversible cytological alterations in single cells upon environmental changes. *Lab Chip* **7**, 71–76 (2007).
7. Wang, X. *et al.* Enhanced cell sorting and manipulation with combined optical tweezer and microfluidic chip technologies. *Lab Chip* **11**, 3656–62 (2011).
8. Guck, J. *et al.* The optical stretcher: a novel laser tool to micromanipulate cells. *Biophys. J.* **81**, 767–84 (2001).

9. Ligler, F. S. & Kim, J. S. *The Microflow Cytometer*. (Pan Stanford Publishing Pte. Ltd.: Singapore, 2010).
10. Boer, G. *et al.* Combining multiple optical trapping with microflow manipulation for the rapid bioanalytics on microparticles in a chip. *Rev. Sci. Instrum.* **78**, 116101 (2007).
11. Bragheri, F. *et al.* Optofluidic integrated cell sorter fabricated by femtosecond lasers. *Lab Chip* **12**, 3779–3784 (2012).
12. Chan, J. W. *et al.* Micro-Raman spectroscopy detects individual neoplastic and normal hematopoietic cells. *Biophys. J.* **90**, 648–56 (2006).
13. Janča, J., Halabalová, V., Polásek, V., Vašina, M. & Menshikova, A. Y. Relaxation of microparticles exposed to hydrodynamic forces in microfluidic conduits. *Anal. Bioanal. Chem.* **399**, 1481–1491 (2011).
14. Lincoln, B. *et al.* Reconfigurable microfluidic integration of a dual-beam laser trap with biomedical applications. *Biomed. Microdevices* **9**, 703–710 (2007).
15. Cran-McGreehin, S., Krauss, T. F. & Dholakia, K. Integrated monolithic optical manipulation. *Lab Chip* **6**, 1122–4 (2006).
16. Bellini, N. *et al.* Femtosecond laser fabricated monolithic chip for optical trapping and stretching of single cells. *Opt. Express* **18**, 4679–4688 (2010).
17. Wetzel, F. *et al.* Single cell viability and impact of heating by laser absorption. *Eur. Biophys. J.* **40**, 1109–14 (2011).
18. Sun, H.-B. & Kawata, S. Two-Photon Photopolymerization and 3D Lithographic Microfabrication. *NMR • 3D Analysis • Photopolymerization* **170**, 169–273 (2004).
19. Liberale, C. *et al.* Micro-Optics Fabrication on Top of Optical Fibers Using Two-Photon Lithography. *IEEE Photonics Technol. Lett.* **22**, 474–476 (2010).
20. Malinauskas, M. *et al.* Laser fabrication of various polymer microoptical components. *Eur. Phys. J. Appl. Phys.* **58**, 20501 (2012).
21. Liberale, C. *et al.* Miniaturized all-fibre probe for three-dimensional optical trapping and manipulation. *Nat. Photonics* **1**, 723–727 (2007).
22. Bragheri, F., Minzioni, P., Liberale, C., Di Fabrizio, E. & Cristiani, I. Design and optimization of a reflection-based fiber-optic tweezers. *Opt. Express* **16**, 17647–17653 (2008).
23. Osterman, N. TweezPal – Optical tweezers analysis and calibration software. *Comput. Phys. Commun.* **181**, 1911–1916 (2010).
24. Singer, W., Bernet, S., Hecker, N. & Ritsch-Marte, M. Three-dimensional force calibration of optical tweezers. *J. Mod. Opt.* **47**, 2921–2931 (2000).
25. Malagnino, N., Pesce, G., Sasso, A. & Arimondo, E. Measurements of trapping efficiency and stiffness in optical tweezers. *Opt. Commun.* **214**, 15–24 (2002).
26. Krafft, C., Knetschke, T., Funk, R. H. W. & Salzer, R. Identification of organelles and vesicles in single cells by Raman microspectroscopic mapping. *Vib. Spectrosc.* **38**, 85–93 (2005).
27. Perozziello, G. *et al.* A Fluidic Motherboard for Multiplexed Simultaneous and Modular Detection in Microfluidic Systems for Biological Application. *Micro and Nanosystems* **2**, 227–238.
28. Perozziello, G. *et al.* Microfluidic Devices Modulate Tumor Cell Line Susceptibility to NK Cell Recognition. *Small* **8**, 2886–2894 (2012).
29. Cojoc, G. *et al.* Optical micro-structures fabricated on top of optical fibers by means of two-photon photopolymerization. *Microelectron. Eng.* **87**, 876–879 (2010).
30. Simone, G. *et al.* A facile in situ microfluidic method for creating multivalent surfaces: toward functional glycomics. *Lab Chip* **12**, 1500–7 (2012).

## Acknowledgments

The authors thank R. Catalano for help on sample preparation. This work was partially supported by the project FIRB “Rete Nazionale di Ricerca sulle Nanoscienze ItaNanoNet” (code: RBPR05JH2P\_010) and the project PON “Nuove strategie nanotecnologiche per la messa a punto di farmaci e presidi diagnostici diretti verso cellule cancerose circolanti” (code: PON01\_02782).

## Author contributions

C.L., F.B. and I.C. conceived the experiments. C.L., G.C., F.B., P.M., G.P., L.F. and V.R. performed the experiments. R.L.R. prepared the biological samples. E.D.F. and I.C. coordinated the project. C.L., F.B., P.M. and I.C. wrote the paper. All authors contributed through scientific discussions.

## Additional information

Supplementary information accompanies this paper at <http://www.nature.com/scientificreports>

**Competing financial interests:** The authors declare no competing financial interests.

**License:** This work is licensed under a Creative Commons Attribution-NonCommercial-NoDerivs 3.0 Unported License. To view a copy of this license, visit <http://creativecommons.org/licenses/by-nc-nd/3.0/>

**How to cite this article:** Liberale, C. *et al.* Integrated microfluidic device for single-cell trapping and spectroscopy. *Sci. Rep.* **3**, 1258; DOI:10.1038/srep01258 (2013).